ADVANCES IN ATMOSPHERIC SCIENCES, VOL. 26, NO. 2, 2009, 265–274

Estimates of Anthropogenic CO_2 Uptake in a Global Ocean Model

XU Yongfu*[1] (徐永福) and LI Yangchun[1,2] (李阳春)

[1] *State Key Laboratory of Atmospheric Boundary Layer Physics and Atmospheric Chemistry, Institute of Atmospheric Physics, Chinese Academy of Sciences, Beijing* 100029

[2] *Graduate University of Chinese Academy of Sciences, Beijing* 100049

(Received 1 November 2007; revised 26 May 2008)

ABSTRACT

A global ocean general circulation model (L30T63) is employed to study the uptake and distribution of anthropogenic CO_2 in the ocean. A subgrid-scale mixing scheme called GM90 is used in the model. There are two main GM90 parameters including isopycnal diffusivity and skew (thickness) diffusivity. Sensitivities of the ocean circulation and the redistribution of dissolved anthropogenic CO_2 to these two parameters are examined. Two runs estimate the global oceanic anthropogenic CO_2 uptake to be 1.64 and 1.73 Pg C yr^{-1} for the 1990s, and that the global ocean contained 86.8 and 92.7 Pg C of anthropogenic CO_2 at the end of 1994, respectively. Both the total inventory and uptake from our model are smaller than the data-based estimates. In this presentation, the vertical distributions of anthropogenic CO_2 at three meridional sections are discussed and compared with the available data-based estimates. The inventory in the individual basins is also calculated. Use of large isopycnal diffusivity can generally improve the simulated results, including the exchange flux, the vertical distribution patterns, inventory, storage, etc. In terms of comparison of the vertical distributions and column inventory, we find that the total inventory in the Pacific Ocean obtained from our model is in good agreement with the data-based estimate, but a large difference exists in the Atlantic Ocean, particularly in the South Atlantic. The main reasons are weak vertical mixing and that our model generates small exchange fluxes of anthropogenic CO_2 in the Southern Ocean. Improvement in the simulation of the vertical transport and sea ice in the Southern Ocean is important in future work.

Key words: anthropogenic CO_2, ocean general circulation model, oceanic uptake, ocean storage

Citation: Xu, Y. F., and Y. C. Li, 2009: Estimates of anthropogenic CO_2 uptake in a global ocean model. *Adv. Atmos. Sci.*, **26**(2), 265–274, doi: 10.1007/s00376-009-0265-z.

1. Introduction

Over the past 200 years, human activities, including the burning of fossil fuels and the production of cement, have emitted a large amount of carbon dioxide (CO_2) into the atmosphere, so that the atmospheric CO_2 concentration has increased by about 100 ppmv. In addition to the accumulation of CO_2 in the atmosphere, the ocean has also absorbed a large amount of the emitted CO_2. However, there is still a large uncertainty about the global oceanic uptake of anthropogenic CO_2. Estimating the anthropogenic CO_2 uptake and storage in the ocean is important for understanding the global carbon cycle and for the projection of future atmospheric CO_2 levels and climate change. For more than 20 years, researchers have made great efforts by global surveys and they have obtained many data sets. Many researchers have used these data sets to estimate the storage of the anthropogenic CO_2 at the basin scale and global scale (Gruber, 1998; Sabine et al., 1999, 2002; Key et al., 2004). Due to the limited spatial and temporal coverage, it is still difficult to accurately estimate the anthropogenic CO_2 uptake and storage in the ocean. It has been realized that the only way to project the influences of greenhouse gases on the future climate is to use numerical models. Examinations of these models require the data. Thus, alternative data-based estimates of the current oceanic anthropogenic CO_2 inventories and transports have provided us an insight into the assessment and validation of the models.

Ocean carbon cycle models have been developed

*Corresponding author: XU Yongfu, xyf@mail.iap.ac.cn

over the past 50 years. From the simplest box model (Craig, 1957) to the dynamic-based three-dimensional (3-D) ocean general circulation model (OGCM) (Maier-Reimer and Hasselmann, 1987), great progress has been made. So far there have been many published results about the oceanic CO_2 sink from 3-D carbon cycle models. These carbon cycle models are basically involved with two categories, including the inorganic carbon cycle with associated biological processes. Most early models employed the inorganic carbon cycle due to the lack of sufficient knowledge of the carbon cycle. At that time, spatial descriptions were limited to one or two dimensions. Since Maier-Reimer and Hasselmann (1987) employed a 3-D ocean inorganic carbon model, the 3-D ocean model has been gradually used in the study of the carbon cycle. The 3-D ocean carbon model with biological processes was developed by Bacastow and Maier-Reimer (1990).

A special model for measuring the anthropogenic CO_2 concentration has been widely used to estimate the oceanic CO_2 uptake. Sarmiento et al. (1992) proposed a perturbation approach to estimate the oceanic uptake of anthropogenic CO_2. That approach presumed that the mechanism and rates of the processes affecting the natural cycling of carbon in the ocean are not affected by the anthropogenic CO_2 increase. In fact, anthropogenic CO_2 is taken as a passive tracer that is fully controlled by physical fields in the interior ocean. Thus, the difference in simulated results between models is mainly due to the difference in OGCMs. This type of simulation is often used in the comparison of OGCMs and to estimate the uptake and storage of anthropogenic CO_2. Orr et al. (2001) compared the oceanic uptake of anthropogenic CO_2 in the four 3-D global ocean carbon cycle models. They found that there were some different results from different models, particularly a large difference on the regional scale.

OGCMs started to develop in China 20 years ago. The first simulation of an OGCM was published in 1989 by researchers at the Institute of Atmospheric Physics/the Chinese Academy of Sciences (IAP/CAS). More than 10 years ago, researchers in China began to develop the 1-D and 2-D ocean carbon cycle models. Jin and Shi (2001) employed MOM2 to study the oceanic uptake of anthropogenic CO_2 in terms of the carbon cycle with biological processes. Xing (2000) developed a 3-D ocean carbon cycle model to study the influence of biological processes on the oceanic uptake of atmospheric CO_2. Dong et al. (1994) and Pu and Wang (2001) used the physical fields from the first generation of the IAP OGCM with 4 vertical levels to study the carbon cycle in the Atlantic and Indian Oceans, respectively. According to the previous OGCM structure, one global OGCM was developed by Jin et al. (1999), which was called L30T63. Li and Shi (2005) examined the L30T63 in terms of radiocarbon, including natural and bomb carbon-14. Simulated results from both the natural and bomb carbon-14 reflected the basic feature of oceanic ventilation. Some differences in the distribution of natural ^{14}C were that the inventory and averaged penetration depth of bomb ^{14}C still existed between the simulated results and the data-based estimates. Li et al. (2006, 2007) used CFC-11 to look at how well the L30T63 could simulate the distribution of CFC-11, and discussed the influences of GM90 parameters on the physical fields and the CFC-11 distributions. Their results showed that two parameters in GM90 could obviously affect the distribution of temperature and salinity as well as CFC-11. They concluded from the analysis of the CFC-11 distributions at several sections, that the increase of isopycnal diffusivity generally improved the simulated inventory of CFC-11 in the main storage regions.

This study, built on our previous research, is to use the L30T63 model to estimate the anthropogenic CO_2 uptake and storage. In addition, we will study the impact of the GM90 parameters on the anthropogenic CO_2 distribution. Meanwhile, the L30T63 is examined in terms of comparison in the simulated anthropogenic CO_2 distribution with the data-based estimate.

2. Model description

2.1 *Ocean general circulation model*

The global ocean general circulation model was developed by the State Key Laboratory of Numerical Modeling for Atmospheric Sciences and Geophysical Fluid Dynamics (LASG) of IAP/CAS, which is named L30T63. The detailed description of the model can be found in Jin et al. (1999). The main features in the model include the free surface, the thermodynamic ice process, the penetration of solar radiation, the Richardson number-dependent mixing process in the tropical ocean, and the isopycnal mixing scheme with an eddy-induced transport velocity by Gent and McWilliams (1990) and Gent et al. (1995), which is called the GM90 parameterization. Horizontal and vertical viscosity coefficients are constant independent of depth. Their values are 5.0×10^4 m^2 s^{-1} (30°S–40°N) and 1.0×10^{-3} m^2 s^{-1}, respectively. For the vertical diffusion coefficient, we take it to be a constant of 0.3×10^{-4} m^2 s^{-1}.

The model domain is global from 79°S to 90°N, including the Arctic Ocean. The horizontal discretization is made based on a triangular spectral truncation

with its zonal wave number of 63 (T63), which approximates to a grid size of about $1.875° \times 1.875°$. The vertical is 30 levels, unequally spaced with 12 levels in the upper 300 m. The top level is 25 m thick and the maximum depth is 5600 m. Two numerical experiments are designed. In our Run 1, both isopycnal and thickness (skew) diffusivities are taken to be 1.0×10^3 m^2 s^{-1}; in Run 2 the isopycnal diffusivity is doubled.

The upper level thermohaline and wind stress forcing is derived from the standard monthly mean climatologies. The surface fluxes of temperature T are calculated in terms of observed heat fluxes between the atmosphere and ocean, and the fluxes of salinity S are calculated by restoring the model predicted salinity in the first level to the observations with a time scale of 30 days. All simulations presented here were initialized from the observed annual mean climatological temperature and salinity data of Levitus (Levitus and Boyer, 1994; Levitus et al., 1994). The model was integrated for more than 1200 years. For the simulation of oceanic carbon uptake, we restarted the model integrations from the above equilibrated ocean circulation of the OGCM, and included an additional passive tracer for anthropogenic CO_2 (online).

2.2 *Anthropogenic* CO_2 *model*

The perturbation approach proposed by Sarmiento et al. (1992) is employed in the model. The atmosphere is treated as a well-mixed box. The upper ocean is exchanged with the atmosphere through the interface of the air-sea. The exchange flux of anthropogenic CO_2 can be written as

$$\text{Flux} = S_{\text{g}}(1 - \gamma_{\text{ice}})(\delta p_{\text{CO}_2,\text{a}} - \delta p_{\text{CO}_2,\text{o}}) \,, \qquad (1)$$

where γ_{ice} is the fraction of sea ice cover, $\delta p_{\text{CO}_2,\text{a}}$ and $\delta p_{\text{CO}_2,\text{o}}$ indicate the perturbations of the partial pressure of carbon dioxide in the atmosphere and the ocean, relative to their preindustrial values. Here the year of 1800 is defined as the beginning of the Industrial Revolution. The perturbed total dissolved inorganic carbon (i.e., anthropogenic CO_2 in the ocean) is considered as a passive tracer. The equation proposed by Sarmiento et al. (1992) is used to relate the partial pressure of anthropogenic CO_2 to the total inorganic anthropogenic carbon in the ocean.

The exchange coefficient (S_{g}) of CO_2 at the air-sea interface is equal to the transfer velocity multiplied by the solubility of CO_2. The transfer velocity from Wanninkhof's (1992) equation is a function of wind speed and seawater temperature. The formula with long term wind speed is used in our model. The data of wind speed is from Esbensen and Kushnir (1981). The time history of atmospheric p_{CO_2} is prescribed by using the values at the beginning and middle of every year, which is taken from Enting et al. (1994), with some implemented values from the recent observed data at Mauna Loa. Then, the atmospheric CO_2 values are linearly interpolated into each time step. After more than 1200 years of integration of the circulation model, the anthropogenic CO_2 is taken as a passive tracer to incorporate it into the circulation model. The initial anthropogenic CO_2 concentrations are set to zero in the ocean. The circulation anthropogenic CO_2 model is run from the beginning of 1800 to the end of 1999.

3. Results and discussion

The transport of anthropogenic CO_2 in the interior ocean is basically the same as that of other passive tracers such as CFCs and carbon-14 except for the difference of the air-sea exchange. After anthropogenic CO_2 dissolves into the seawater, its redistributions are fully controlled by the physical fields. Basic characteristics of the model have been discussed in Jin et al. (1999). Overall, the simulated physical fields, including the thermocline and the equatorial currents systems, are basically in agreement with the observations. For instance, the model reproduces the surface distribution and vertical patterns of the temperature and salinity. However, the formation of the simulated Antarctic Bottom water (AABW) is insufficient.

The air-sea exchange of anthropogenic CO_2 is largely driven by the difference of anthropogenic CO_2 concentrations in the atmosphere and the first level of the model ocean. Figure 1 shows the annual mean exchange fluxes of anthropogenic CO_2 in 1994. In the area with strong vertical velocity (e.g., in the equatorial Pacific upwelling region), the anthropogenic CO_2 flux is normally large (Sarmiento et al., 1992). For instance, both runs show the large flux in the eastern equatorial Pacific region, with the largest one being 0.9 mol m^{-2} yr^{-1}. Model simulations also show that the western North Atlantic, western North Pacific, and Southern Ocean are important sinks of anthropogenic CO_2, because of strong vertical advection and convection mixing that rapidly transport the absorbed anthropogenic CO_2 from the surface to deeper waters. The uptake rate of anthropogenic CO_2 in the western North Atlantic can reach 2 mol m^{-2} yr^{-1}. There are some differences in these regions between the two runs. Great isopycnal diffusivity (Run 2) enhances the transport of anthropogenic CO_2 in the western North Atlantic, western North Pacific, and the region near 60°S.

While the absorbing region of anthropogenic CO_2 is mainly determined by vertical movement, the surface distribution of anthropogenic CO_2 concentration is largely affected by ocean surface currents. It can be seen in Fig. 2 that except for the Arctic Ocean and

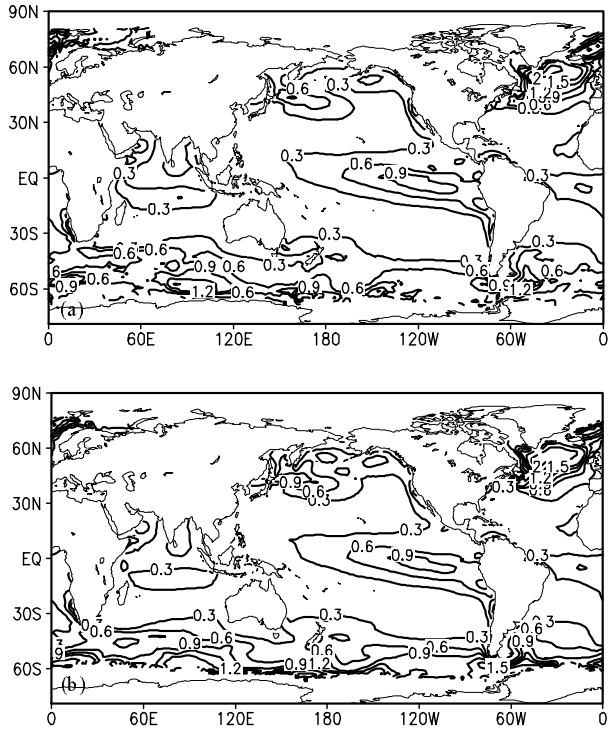

Fig. 1. Annual mean distribution of sea-air exchange fluxes (mol m^{-2} yr^{-1}) of anthropogenic CO_2 in 1994: (a) Run 1 and (b) Run 2.

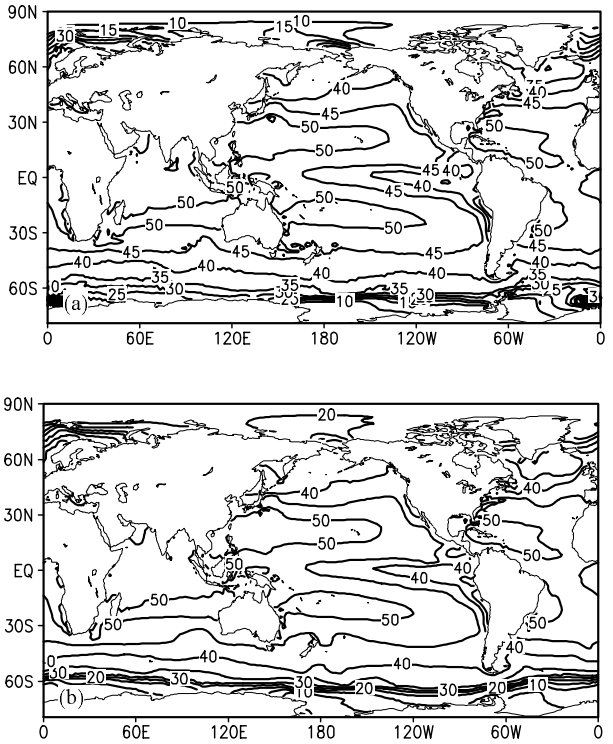

Fig. 2. Annual mean distribution of anthropogenic CO_2 (μmol kg^{-1}) at 12.5 m in 1994: (a) Run 1 and (b) Run 2.

the Southern Ocean, where anthropogenic CO_2 concentrations are low because of sea ice cover, in the equatorial region, particularly in the equatorial eastern Pacific Ocean, there is a low value of 40 μmol kg^{-1} for anthropogenic CO_2 due to strong upwelling. The anthropogenic CO_2 absorbed in the eastern equatorial region is transported along with the equatorial surface current to the west, accumulates near the coast, and then moves polewards. Meanwhile, the anthropogenic CO_2 absorbed in the western North Pacific and western North Atlantic is transported along with the subpolar gyre to the south and then along with the west wind drift to the east, resulting in west- to-east increases in higher latitudes and west-to-east decreases in middle and lower latitudes. As a result, surface anthropogenic CO_2 is accumulated in the subtropical regions. As shown in Fig. 2, anthropogenic CO_2 concentrations can reach 50 μmol kg^{-1} in the subtropical regions of three ocean basins. The 50 μmol kg^{-1} contour covers the largest area in the Pacific. This spatial distribution pattern is consistent with the data-based estimate by Key et al. (2004). The data-based results show that anthropogenic CO_2 in the Atlantic Ocean is much higher than that in other basins. However, the high concentration in the Atlantic Ocean is controversy (Key et al., 2004). Although the data-based results give a small concentration of anthropogenic CO_2 in the Southern Ocean, our simulations still underestimate the data-based values.

Figure 3 presents the distribution of simulated anthropogenic CO_2 at 151°W. According to the data-based results (from http://cdiac.ornl.gov), the vertical distribution of anthropogenic CO_2 at this section is quite similar to the simulated results with a "W" structure, in which the deepest penetration is near 40° in both the South and North Pacific, whereas the shallowest penetrations are in both higher latitudes and near 10°N. Our model successfully reproduces these observed features. Some differences in penetration depth exist between the two runs. For example, the 5 μmol kg^{-1} contour in Run 2 penetrates into the deepest level of 1350 m at 40°S, which is in good agreement with the data-based estimate, whereas in Run 1 the same contour can only penetrate into the deepest level of 1170 m and the location is 8° to the south, compared with Run 2 and the data-based results. In addition, the deepest penetration of the 5 μmol kg^{-1} contour in the North Pacific is about 820 m in Run 2, slightly larger than 800 m in Run 1, but much smaller than the data-based estimate of 1100 m. This demonstrates that an increase in isopycnal diffusivity cannot obviously increase the storage of anthropogenic CO_2

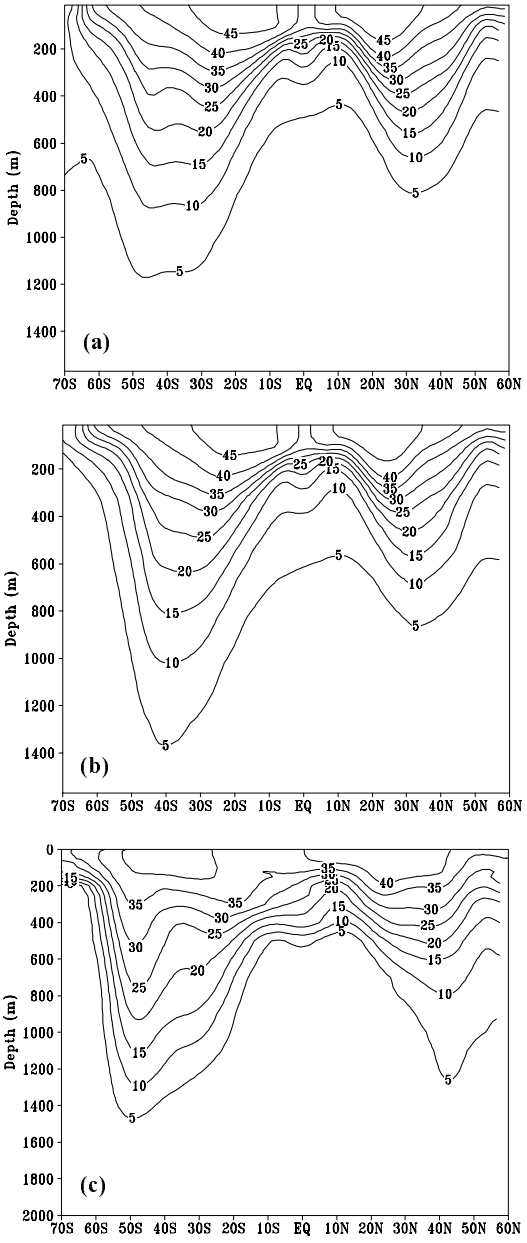

Fig. 3. Annual mean distribution of anthropogenic CO_2 (μmol kg^{-1}) at 151°W in 1991: (a) Run 1, (b) Run 2, and (c) observations.

in some regions. As pointed out by Xu et al. (2007), the increase of isopycnal diffusivity can enhance the storage in the western North Pacific but does not help much in the eastern North Pacific.

In the Atlantic, there were a few cruises in 1980s, including TTO (Transient Tracers in the Ocean, 1981–1982) and SAVE (South Atlantic Ventilation Experiment, 1987–1988). Using these cruise data sets, Gruber (1998) has given distributions of anthropogenic CO_2 at some sections, in which one section in the western Atlantic includes the observed data that was taken from a meandering cruise in the region from 60°W to 20°W. We took the regional average for comparison. Figure 4 presents the simulated results from the two runs. It can be seen that the pattern is quite similar to that along 151°W. For example, the penetration depth of the contours with values larger than 5 μmol kg^{-1} deepens from near the equator to the mid-latitudes, showing a relatively shallow depth at 10°N, and a deep depth near 40°S and in the subtropical regions. This demonstrates that the transport path of anthropogenic CO_2 determined by the similar structure of an isopycnal surface in the different basins is basically consistent. However, due to strong convection in the western North Atlantic, the 5 μmol kg^{-1} contour can reach the deepest penetration below 3000 m in the region north of 50°N, which is quite different from that along 151°W. The simulated result is in agreement with the data-based estimate by Gruber (1998). Data-based results also show that the largest penetration depth of the 5 μmol kg^{-1} contour is about 1800 m at 40°S in the Southern Hemisphere. Although our model generates the correct position of the deepest penetration, the model underestimates the penetration depth. The model simulation shows that Run 2 is better than Run 1, with the deepest penetration being 1350 m and 1120 m, respectively. It should be pointed out that the penetration depth in the region north of 40°N in Run 2 is shallower than in Run 1. This is because the increase of isopycnal diffusivity affects the transport of both passive tracers and active tracers (temperature and salinity) so that the large isopycnal diffusivity enhances the stability of stratification, therefore weakening convection (Li et al., 2007). Additionally, the vertical transport of anthropogenic CO_2 caused by convection is weakened in that region in Run 2 relative to Run 1. In general, the simulated result along this section is in agreement with the data-based estimate. The influence of isopycnal diffusivity on the different processes is well reflected in this section.

Figure 5 presents the distribution of anthropogenic CO_2 along 92°E of the Indian Ocean in February 1995. Figure 5c was drawn according to the data obtained from http://cdiac.ornl.gov. The vertical distribution of anthropogenic CO_2 at this meridional section in the Indian Ocean is quite similar to that in the Pacific Ocean and Atlantic Ocean. The penetration is shallow in the region south of 60°S and in the equatorial region, and deep in the region of 40°–50°S. This reflects the transport of passive tracers along the isopycnal surfaces. Although our model cannot reproduce well the high values of anthropogenic CO_2 at the subsurface layer near 40°S, which is similar to the results

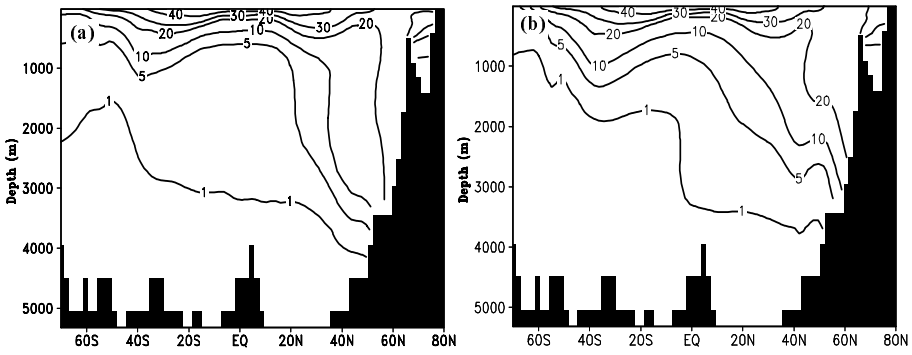

Fig. 4. Anthropogenic CO_2 (μmol kg^{-1}) distribution in the region of 20°–60°W in 1986: (a) Run 1 and (b) Run 2.

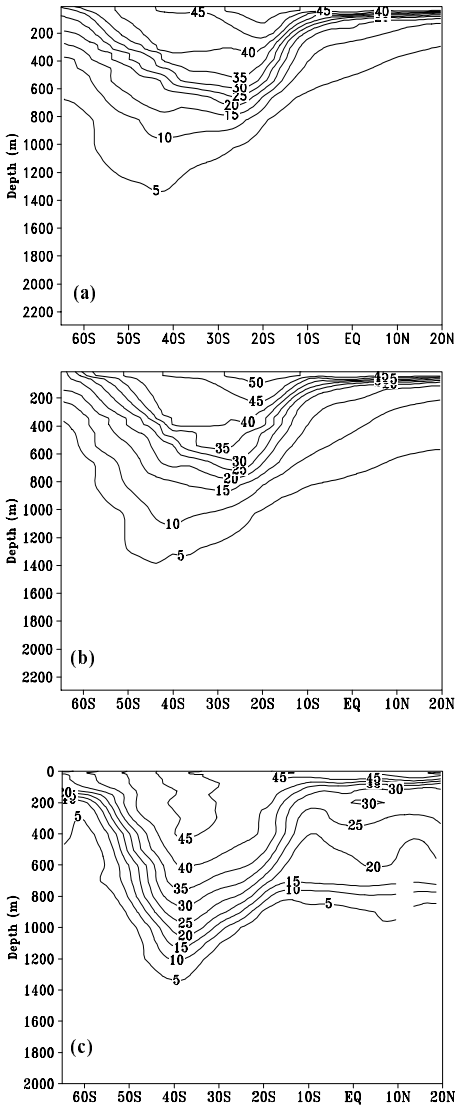

Fig. 5. Anthropogenic CO_2 (μmol kg^{-1}) distribution at 92°E in February 1995: (a) Run 1, (b) Run 2, and (c) observations.

from four models compared by Orr et al. (2001), the main distribution characteristics are in agreement with data-based estimates (Sabine et al., 1999). The difference between the two runs is small in this section. The contours in the region north of 10°S are more dispersive in Run 2 than in Run 1. In the region south of 50°S the contours in Run 2 are sharper than those in Run 1. These characteristics in Run 2 are much closer to the data-based estimates than those in Run 1.

Figure 6 shows the anthropogenic CO_2 inventory from the two runs. It can be seen that just as the presentation at sections, storing regions are mainly located in the subtropical regions of both hemispheres. However, in the northern hemisphere, different physical processes lead to the differences in the location and magnitude of a high anthropogenic CO_2 inventory between the North Atlantic and the North Pacific. The inventory in the subtropical region of the North Pacific is about 20 mol m^{-2} in 1994, mainly located in the region of 20°–40°N. However, the inventory can reach as high as 70 mol m^{-2} in the western North Atlantic because strong convection makes anthropogenic CO_2 reach the bottom of the ocean, as seen in Fig. 4. The location is relatively to the North. These distribution features are in agreement with data-based estimates by Key et al. (2004) who used the observed data sets from WOCE (World Ocean Circulation Experiment) and JGOFS (Joint Global Ocean Flux Study).

In the southern hemisphere, according to the estimate by Key et al. (2004), the difference in the main storage of anthropogenic CO_2 among basins is not as obvious as that in the northern hemisphere. The high inventory in both the Indian Ocean and the Atlantic Ocean appears to be in the region of 25°–45°S, with the highest value being more than 40 mol m^{-2}. The high inventory in the Pacific is located relatively to the south. The area with the inventory more than 40 mol m^{-2} is much smaller than that in the other two basins. We notice that the storing region from our si-

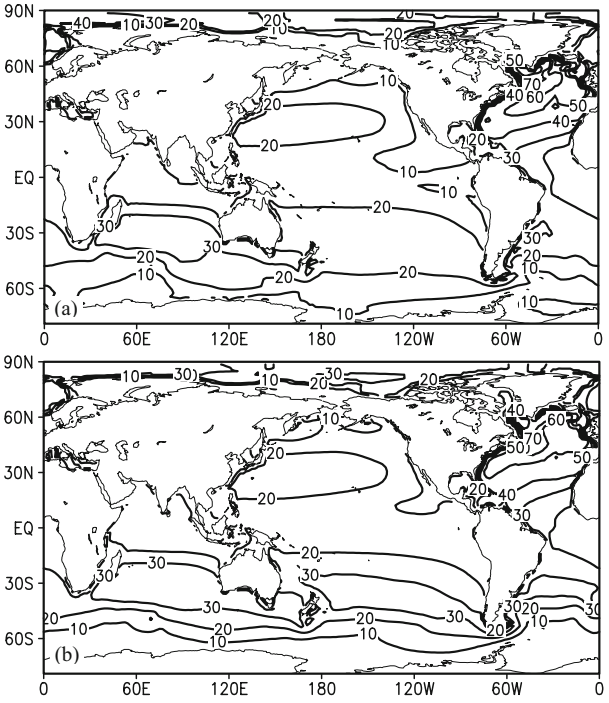

Fig. 6. Distribution of anthropogenic CO_2 column inventory (mol m^{-2}) in 1994: (a) Run 1 and (b) Run 2.

mulations is quite consistent with the data-based estimate, but the magnitude is much smaller relative to the data-based value. The highest inventory in the South Pacific from Run 2 is 30 mol m^{-2}, which is smaller than the data-based estimate. The high inventory from Run 2 is larger than that from Run 1. It has been realized that the anthropogenic CO_2 in the subtropical regions of the Southern Hemisphere is mainly from the Southern Ocean. Considering the surface distribution of anthropogenic CO_2 in Fig. 2, we can presume why the position of the simulated inventory is correct but the magnitude is too small. One of the reasons is that the simulated uptake in the southern ocean is too small. It can be seen in Fig. 1 that the simulated annual mean air-sea exchange flux is close to 0 in the region south of 60°S. This is because our simulations give rise to almost a permanent ice cover in the region of 60°–70°S, which limits the exchange of anthropogenic CO_2 between the atmosphere and ocean according to Eq. (1). Furthermore, our model under predicts the vertical transport in the Subantarctic Zone, which results in underestimating the uptake of anthropogenic CO_2, because GM90 generally tends to weaken the convection. In fact, there is a strong convection in the Subantarctic Zone, as pointed out by Wang and Matear (2001) and the winter mixed layer depth can reach 600 m in the Subantarctic Zone. In order to improve our simulations of anthropogenic CO_2 storage in the southern hemisphere, the main focus of future work is to improve the simulation of vertical transport and sea ice in the Southern Ocean.

In order to perceivably compare with data-based estimates, we respectively calculate the zonal mean anthropogenic CO_2 inventory in different basins. All data-based results are obtained from Fig. 9 of Sabine et al. (2002), in which results in the Pacific Ocean, the Atlantic Ocean, and the Indian Ocean were obtained by Sabine et al. (2002), Gruber (1998), and Sabine et al. (1999), respectively. For consistency with the observations, we used the simulated results from 1994 for the Pacific Ocean, from 1995 for the Indian Ocean, and from 1986 for the Atlantic Ocean. The data-based inventory in Fig. 7 indicates that the largest inventory in the Southern Hemisphere appears to be near 50°S in the Pacific Ocean, near 40°S in the Atlantic Ocean, and near 35°S in the Indian Ocean. As discussed above, the largest inventory in the Pacific Ocean is located to the south relative to other basins, and its value is about 35 mol m^{-2}, smaller than 49 mol m^{-2} in the Atlantic Ocean, and 40 mol m^{-2} in the Indian Ocean. The trend of change in the inventory from our simulations is in agreement with the data-based one. Although the location of the simulated maximum inventory is quite consistent with the data-based one, the value is smaller than the data-based inventory. Because the simulated surface anthropogenic CO_2 concentrations are much lower than the data-based concentrations, the simulated inventory in the whole Atlantic Ocean is 20 mol m^{-2} smaller than the data-based estimate. In the Southern Hemisphere of the other two basins, the difference in the inventory between the simulations and the data-based estimate is generally less than 5 mol m^{-2}. As pointed out above, the main reason for our low inventory is that the absorbing ability in the Southern Ocean is weakened in our model. The simulated inventory in the Northern Hemisphere is basically in agreement with the data-based estimate. In the North Pacific the difference in the largest inventory between Run 2 and the data-based result is less than 2 mol m^{-2}. However, the location is quite different (Fig. 7a). In the North Atlantic, although our model under predicts the data-based inventory, the trend of change is consistent with the data-based results. Both the simulated results and the data-based estimates reflect that the inventory in the higher latitudes is larger than that in the subtropical regions, except for the region north of about 60°N because of strong convection taking place there. Model simulations show that the inventory in Run 2 is larger than in Run 1. This is in accord with our discussion of the vertical distribution. Increasing isopycnal diffusivity can increase the penetration depth of anthro-

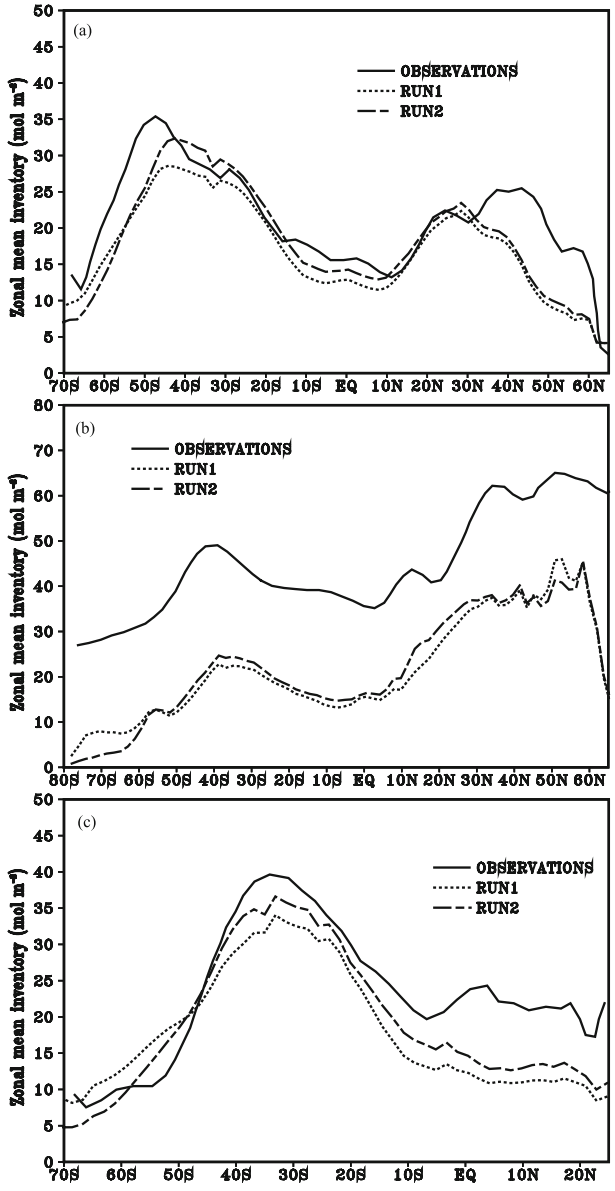

Fig. 7. Zonal mean anthropogenic CO_2 inventory (mol m^{-2}) in the (a) Pacific, (b) Atlantic, and (c) Indian Ocean.

pogenic CO_2.

Based on the above discussed inventory of anthropogenic CO_2, we can calculate the total inventory on both the basin scale and the global scale. Many researchers have estimated the total oceanic inventories of anthropogenic CO_2 in terms of both observed data and model results. Using observed data sets, Sabine et al. (2002) estimated the total anthropogenic CO_2 inventory of 44±5 Pg C in the Pacific Ocean around 1994. Our Runs 1 and 2 estimate an inventory of 40.2 and 43.4 Pg C, respectively, which is in good agreement with Sabine et al. (2002)'s estimate. Gruber (1998) estimated that the North Atlantic contained about 22±5 Pg C in 1982, and the South Atlantic about 18±4 Pg C in 1989, whereas our Runs 1 and 2 estimate an inventory of 15.2 and 17.2 Pg C in the North Atlantic in 1982, and 9.3 and 10.7 Pg C in the South Atlantic in 1989, respectively. The simulated results underestimate the data-based inventory by about 26% in the North Atlantic and about 44% in the South Atlantic. Sabine et al. (1999) estimated the inventory of 20.3±3 Pg C in the Indian Ocean around 1995, whereas our Runs 1 and 2 estimate the inventory of 17.2 and 18.5, respectively, which is within the data-based range. Sabine et al. (2004) further estimated a global oceanic anthropogenic CO_2 sink for the period 1800–1994 of 118±19 Pg C, which is much larger than our estimates of 86.8 and 92.7 Pg C. The total inventory from Run 2 is larger than that from Run 1, reducing the difference with the data-based estimate. Therefore, the use of relatively large isopycnal diffusivity can improve the simulated results in the L30T63 model, which is also demonstrated in the simulation of CFC-11 (Li et al., 2007).

In terms of the exchange flux of anthropogenic CO_2, we can calculate the total uptake of anthropogenic CO_2 on both the basin scale and the global scale. Our simulations show that the global oceanic uptake of anthropogenic CO_2 from Runs 1 and 2 is 1.45 and 1.53 Pg C yr^{-1} for the 1980–1989 average, and 1.64 and 1.73 Pg C yr^{-1} for the 1990–1999 average. Since Sarmiento et al. (1992) proposed the perturbation approach and estimated that the global ocean was taking up 1.9 Pg C yr^{-1} of anthropogenic CO_2 in the 1980s, researchers have continued to use different models to estimate the ocean budget of anthropogenic CO_2. Orr et al. (2001) compared 4 different OGCMs in the simulations of anthropogenic CO_2 and bomb carbon-14. Estimates of the global ocean uptake of anthropogenic CO_2 from four 3-D models were within 1.85±0.35 Pg C yr^{-1} in the 1980s. Thomas et al. (2001) proposed an estimate of the oceanic anthropogenic CO_2 inventory as well as its time history according to atmospheric p_{CO_2} and age spectra to describe the water mass ventilation history, and obtained a high global oceanic uptake of 3.9 Pg C yr^{-1} for the year 1999. McNeil et al. (2003) used a global CFC data set to indicate a global oceanic net uptake of 1.6 and 2.0 ± 0.4 Pg C yr^{-1} of anthropogenic CO_2 in the 1980s and 1990s, respectively. They further pointed out that most ocean models were overestimating the oceanic anthropogenic CO_2 uptake over the past two decades. It is obvious that our model estimates are near the low bound of other model estimates.

Recently, Waugh et al. (2006) employed both the transit time distribution (TTD) method, applied to

global measurements of CFC-12, and the directed simulated anthropogenic CO_2 to estimate the global inventory of anthropogenic CO_2, and suggested an inventory range of 94–121 Pg C in 1994. Using a Green's function inversion method that combines the data-based estimates of anthropogenic CO_2 with the information about ocean transport and mixing from 10 OGCMs, Mikaloff Fletcher et al. (2006) obtained a global uptake of 2.2±0.25 Pg C yr^{-1} for 1995. Most recently, Sweeney et al. (2007) used the updated database of dissolved inorganic carbon, ^{14}C and a suit of OGCMs in an inverse mode to obtain a net air-sea flux estimate of 1.3±0.5 Pg C yr^{-1} for 1995. After accounting for the carbon transferred from rivers to the deep ocean, they estimated an oceanic uptake of 1.8±0.5 Pg C yr^{-1}. It is obvious that a large difference still exists between the estimates by different researchers. Goodwin et al. (2007) presented a theory for the ocean-atmosphere portioning of anthropogenic CO_2 on centennial timescales, and suggested a restriction to a total carbon emission of 700 Pg C to achieve the atmospheric CO_2 stabilization at present-day transient levels.

4. Conclusions

This study has employed a global ocean circulation carbon cycle model called L30T63 to simulate the uptake and storage of anthropogenic CO_2 in the ocean. Two numerical experiments called Runs 1 and 2 were designed for the sensitivity of anthropogenic CO_2 uptake to GM90 parameters.

Our simulations gave rise to an average oceanic anthropogenic CO_2 uptake rate of 1.45 (Run 1) and 1.63 Pg C yr^{-1} (Run 2) for the period 1980–1989, and 1.64 (Run 1) and 1.73 Pg C yr^{-1} (Run 2) for the period 1990–1999. Compared with data-based and other model-based uptakes, our model gives rise to a low bound. Our model estimates that the global ocean contained 86.8 (Run 1) and 92.7 (Run 2) Pg C of anthropogenic CO_2 at the end of 1994, which is smaller than the data-based estimates. The main difference in the total oceanic uptake between our simulations and data-based estimates appears to be in the Southern Ocean. According to the comparison of individual basins, the total inventory in the Pacific Ocean obtained from our model is in good agreement with the data-based estimate, whereas a large difference in the Atlantic Ocean exists, particularly in the Southern Atlantic.

The large exchange flux generally appears to be in the regions where there is strong convection or vertical movement. The western North Pacific, western North Atlantic, and the eastern equatorial Pacific are main regions of taking up anthropogenic CO_2. The largest air-sea exchange flux can reach over 2 mol m^{-2} yr^{-1} in the western North Atlantic. High surface anthropogenic CO_2 concentrations are located in the subtropical regions, with the largest value being 50 μmol kg^{-1} in 1994. In terms of three meridional sections of anthropogenic CO_2 distributions, simulated results are compared with the data-based estimates. The deepening and shallowing of anthropogenic CO_2 penetrations are well produced, compared with the data-based estimates at all three sections.

The increase of isopycnal diffusivity can generally improve the simulated results. Use of large isopycnal diffusivity enhances the exchange flux of anthropogenic CO_2 in the western North Pacific and western North Atlantic. The storage of anthropogenic CO_2 in the subtropical regions of the Southern Hemisphere is increased due to the increase of isopycnal diffusivity, which is much closer to the data-based estimates. Although the uptake rate of anthropogenic CO_2 can be increased in the model with a large isopycnal diffusivity, the model-estimated inventory and uptake are still smaller, compared with the data-based estimates. This is mainly involved with the simulation of vertical transport and sea ice, which needs to be improved in the future. Large uncertainties are included in both model and data-based results. The reduction of uncertainties has been a main subject for the carbon cycle research community.

Acknowledgements. The authors would like to thank Dr. Xiujun Wang for her detailed review and comments that greatly helped us for the improvement of our manuscript. We would also like to thank an anonymous reviewer for his constructive comments. This work was supported by the Knowledge Innovation Program of the Chinese Academy of Sciences (KZCX-2-YW-218), the National Natural Science Foundation of China (40730106), and the Key Frontier Project of the Institute of Atmospheric Physics (IAP07114).

REFERENCES

Bacastow, R., and E. Maier-Reimer, 1990: Ocean-circulation model of the carbon cycle. *Climate Dyn.*, **4**, 95–125.

Craig, H, 1957: The natural distribution of radiocarbon and the exchange time of carbon dioxide between atmosphere and sea. *Tellus*, **9**, 1–17.

Dong, T. L., M. X. Wang, and R. Z. Liu, 1994: Two-dimensional atmospheric CO_2-Atlantic carbon cycle model. *Chinese J. Atmos. Sci.*, **18**, 631–640. (in Chinese)

Enting, I. G., T. M. Wigley, and M. Heimann, 1994: Future emissions and concentration of carbon dioxide:

Key ocean/atmosphere/land analysis. CSIRO Division of Atmospheric Research Technical Paper No. 31, CSIRO, Australia, 120pp.

Esbensen, S. K., and Y. Kushnir, 1981: The heat budget of the global ocean: An atlas based on estimates from surface marine observations. Rept. 29, Climate Research Institute, Oregon State University, Corvallis, 27pp.

Gent, P. R., and J. C. McWilliams, 1990: Isopycnal mixing in ocean circulation models. *J. Phys. Oceanogr.*, **25**, 463–474.

Gent, P. R., J. Willebrand, T. J. McDougall, and J. C. McWilliams, 1995: Parameterizing eddy-induced tracer transports in ocean circulation models. *J. Phys. Oceanogr.*, **25**, 463–474.

Goodwin, P., R. G. Williams, M. J. Follows, and S. Dutkiewicz, 2007: Ocean-atmosphere partitioning of anthropogenic carbon dioxide on centennial timescales. *Global Biogeochemical Cycles*, **21**, GB1014, doi: 10.1029/2006GB002810.

Gruber, N., 1998: Anthropogenic CO_2 in the Atlantic Ocean. *Global Biogeochemical Cycles*, **12**, 165–191.

Jin, X., and G. Y. Shi, 2001: The role of biological pump in ocean carbon cycle. *Chinese J. Atmos. Sci.*, **25**, 683–688. (in Chinese)

Jin, X. Z., X. H. Zhang, and T. J. Zhou, 1999: Fundamental framework and experiments of the third generation of IAP/LASG world ocean general circulation model. *Adv. Atmos. Sci.*, **16**, 197–215.

Key, R. M., and Coauthors, 2004: A global ocean carbon climatology: Results from Global Data Analysis Project (GLODAP). *Global Biogeochemical Cycles*, **18**, doi: 10.1029/2004GB002247.

Levitus, S., and T. P. Boyer, 1994: World Ocean Atlas 1994, Volume 4: Temperature. NOAA Atlas NESDIS 4, 117pp.

Levitus, S., R. Burgett, and T. P. Boyer, 1994: World Ocean Atlas 1994, Volume 3: Salinity. NOAA Atlas NESDIS 3, 99pp.

Li, Q. Q., and G. Y. Shi, 2005: Simulation of ^{14}C in IAP/LASG L30T63 ocean model. *Acta Meteorologica Sinica*, **19**, 436–446.

Li, Y. C., Y. F. Xu, L. Zhao, and M. X. Wang, 2006: Preliminary study of the simulated distribution of CFC-11 in the global ocean circulation model. *Chinese J. Atmos. Sci.*, **30**(4), 671–681. (in Chinese)

Li, Y. C., Y. F. Xu, L. Zhao, and M. X. Wang, 2007: Sensitivity of CFC-11 uptake in a global ocean model to subgrid-scale mixing parameterizations. *Acta Oceanologica Sinica*, **29**(3), 31–38. (in Chinese)

Maier-Reimer, E, and K. Hasselmann, 1987: Transport and storage of CO_2 in the ocean—An inorganic ocean-circulation carbon cycle model. *Climate Dyn.*, **2**, 63–90.

McNeil, B. I., R. J. Matear, R. M. Key, J. L. Bullister, and J. L. Sarmiento, 2003: Anthropogenic CO_2 uptake by the ocean based on the global chlorofluorocarbon data sea. *Science*, **299**, 235–239.

Mikaloff Fletcher, S. E., and Coauthor, 2006: Inverse estimates of anthropogenic CO_2 uptake, transport, and storage by the ocean. *Global Biogeochemical Cycles*, **20**, GB2002, doi: 10.1029/2005GB002530.

Orr, J., and Coauthors, 2001: Estimates of anthropogenic carbon uptake from four 3-D global ocean models. *Global Biogeochemical Cycles*, **15**, 43–60.

Pu, Y. F., and M. X. Wang, 2001: An ocean carbon cycle model, Part II: Simulation analysis on the Indian Ocean. *Climatic and Environmental Research*, **6**, 67–76. (in Chinese)

Sabine, C. L., and Coauthors, 2002: Distribution of anthropogenic CO_2 in the Pacific Ocean. *Global Biogeocheical Cycles*, **16**(4), doi: 10.1029/2001GB011639.

Sabine, C. L., R. M. Key, K. M. Johnson, F. J. Millero, J. L. Sarmiento, D. W. R. Wallace, and C. D. Winn, 1999: Anthropogenic CO_2 inventory of the Indian Ocean. *Global Biogeochemical Cycles*, **13**(1), 179–198.

Sabine, C. L., and Coauthors, 2004: The oceanic sink for anthropogenic CO_2. *Science*, **305**, 367–371.

Sarmiento, J. L., J. C. Orr, and U. Siegenthaler, 1992: A perturbation simulation of CO_2 uptake in an ocean general circulation model. *J. Geophys. Res.*, **97**, 3621–3645.

Sweeney, C., E. Gloor, A. R. Jacobson, R. M. Key, G. McKinley, J. L. Sarmiento, and R. Wanninkhof, 2007: Constraining global air-sea gas exchange for CO_2 with recent bomb ^{14}C measurements. *Global Biogeochemical Cycles*, **21**, GB2015, doi: 10.1029/2006GB002784.

Thomas, H., M. H. England, and V. Ittekkot, 2001: An off-line 3D model of anthropogenic CO_2 uptake by the oceans. *Geophys. Res. Lett.*, **28**, 547–550.

Wanninkhof, R., 1992: Relationship between wind speed and gas exchange over the ocean. *J. Geophys. Res.*, **9**, 7373–7382.

Waugh, D. W., T. M. Hall, B. I. McNeil, R. Key, and R. J. Matear, 2006: Anthropogenic CO_2 in the oceans estimated using transit time distributions. *Tellus*(B), **58**(5), 376–389.

Wang, X., and R. J. Matear, 2001: Modeling the upper ocean dynamics in the Subantarctic and Polar Frontal Zones in the Australian sector. *J. Geophys. Res.*, **106**, 31511–31524.

Xing, R. N., 2000: A three-dimensional world ocean carbon cycle model with ocean biota. *Chinese Journal Atmospheric Sciences*, **24**, 333–340. (in Chinese)

Xu, Y. F., L. Zhao, and Y. C. Li, 2007: Numerical simulations of uptake of anthropogenic CO_2 in the North Pacific. *Chinese Journal of Geophysics*, **50**(2), 404–411.